frontiers | Frontiers in Materials

TYPE Original Research
PUBLISHED 27 February 2024
DOI 10.3389/fmats.2024.1363138

OPEN ACCESS

EDITED BY
Zhiyong Gao,
Central South University, China

REVIEWED BY
Lin Wei,
Lam Research, United States
Yu Yang,
Applied Materials, United States

*CORRESPONDENCE
Muhammad Faizan Nazar,
faizan.nazar@ue.edu.pk
Zaka Ullah,
zaka.ullah@ue.edu.pk

RECEIVED 29 December 2023
ACCEPTED 05 February 2024
PUBLISHED 27 February 2024

CITATION
Zafar S, Nazar MF, Siddique MY, Haider S, Alam K, Saleem MA, Shaukat S, Abd Ur Rahman HM and Ullah Z (2024), Formulation and evaluation of ophthalmic microemulsion for enhanced topical administration of brinzolamide.
Front. Mater. 11:1363138.
doi: 10.3389/fmats.2024.1363138

Formulation and evaluation of ophthalmic microemulsion for enhanced topical administration of brinzolamide

Sehrish Zafar[1], Muhammad Faizan Nazar[1]*, Muhammad Yasir Siddique[2], Sajjad Haider[3], Kamran Alam[4], Muhammad Atif Saleem[2], Saadia Shaukat[5], Hafiz Muhammad Abd Ur Rahman[5] and Zaka Ullah[6]*

[1]Department of Chemistry, Division of Science and Technology, University of Education, Lahore, Pakistan, [2]Department of Chemistry, University of Gujrat, Gujrat, Pakistan, [3]Chemical Engineering Department, College of Engineering, King Saud University, Riyadh, Saudi Arabia, [4]Department of Chemical Engineering Materials Environment Sapienza University of Rome, Rome, Italy, [5]Department of Chemistry, Government College Women University Sialkot, Sialkot, Pakistan, [6]Department of Physics, Division of Science and Technology, University of Education, Lahore, Pakistan

Microemulsions (μEs) are more effective than conventional formulations for ophthalmic use due to their optical transparency, thermodynamic stability, structural flexibility and higher bioavailability. In addition, μE formulations can increase the water solubility of the drug and improve drug absorption in the eye. Herein, we report the development of three new biocompatible μE formulations containing an antihypertensive drug brinzolamide (BZD) and their evaluation for topical ocular administration. For this, Formulations A, B and C were optimized using an appropriate ratio of isopropyl myristate (IPM) as oil phase, water as aqueous phase and 2-propanol as co-surfactant, while Tween-80, Tween-20 and Tween-60 were selected as surfactant for each formulation, respectively. Preliminary, pseudoternary phase diagrams were delineated and then electrical conductivity and optical microscopy were used to establish optimal formulation for each μE to upheld the appropriate amount of BZD, i.e., 2.0 wt%, 2.0 wt%, and 1.0 wt% in formulation A, B and C, respectively. Dynamic light scattering demonstrated very fine monomodal assembly of BZD-μE nanodroplets (~50 nm), while FTIR analysis showed effective encapsulation of BZD into hydrophobic microenvironment with no observable chemical interaction between BZD and μE excipients, which was further verified by the peak-to-peak concomitant measurement of fluorescence. Further, *in-vitro* release of BZD-μE showed enhanced and persistent topical ocular administration (>99%) within 10 h demonstrating the appropriate formulation for topical instillation.

KEYWORDS

microemulsion, topical, ocular, monomodal, nanodroplets

Introduction

Glaucoma is a serious chronic disease that causes weakening of the retinal nerves and ganglion cells, leading to pathophysiological changes in the structure of the eye. Glaucoma

can cause vision loss and, if left untreated, lead to complete blindness. Intraocular pressure is the main cause of the development of glaucoma due to the increased production of aqueous humour (Loiselle et al., 2020). Brinzolamide (BZD) is used as the first-line drug for the treatment of glaucoma (Silver and Group, 2000). BZD is an ocular carbonic anhydrase inhibitor and reduces the production of aqueous humour and directly lowers intraocular pressure when applied to the target area (Eissa, 2016; Choradiya and Patil, 2022). BZD being a lipophilic drug, has very poor solubility in aqueous media and the commercial BZD formulation contains only 1% of BZD in the water suspension. This suspension has many side effects on the eyes, including blurred vision, pain and dry eyes, and this limitation significantly reduces the importance of BZD as an ophthalmic medication (Gohil et al., 2020). Apart from the side effects, it has other limitations like small residence time, poor bioavailability and pre-corneal drug loss. The delivery of drugs to the eye is a challenging process due to the unique physiology and anatomy of the eye (Urtti, 2006).

Topical administration of eye drops is the most common method of treating eye diseases due to the presence of blood–retinal barrier that makes systemic drug administration ineffective. Various studies have been conducted to develop novel methods such as micellar systems, contact lenses, hydrogels and microemulsions (μE) that can increase the bioavailability of the drug to the eye (Abd El Wahab et al., 2022; Qadri et al., 2022a; Saleem et al., 2023). μE has emerged as an effective alternative to conventional ocular drug delivery methods (Grampurohit et al., 2011; Patel et al., 2013; Nazar et al., 2018). μEs are being explored as an effective drug delivery vehicle for ophthalmic medications, offering advantages such as structural flexibility, optical transparency, thermodynamic stability, enhanced solubilization, higher bioavailability and ease of formation (Constantinides, 1995; Gasco, 1997; Tenjarla, 1999; Kantaria et al., 2003).

μEs are stable liquid mixtures containing oil and aqueous phases as well as surfactants and co-surfactants and are isotropic and clear in appearance (Saleem et al., 2020). Their formation is easy compared to ordinary emulsions and does not require high shear conditions (Danielsson, 1981; Yuan et al., 2006; Narang et al., 2007). Depending on the composition of the formulation, there are three types of μE. In the oil-in-water (o/w) μE, there is a continuous water phase in which oil droplets are dispersed. In contrast, the dispersion of water droplets in the continuous oil phase leads to the formation of water-in-oil (w/o) μE (Yasir Siddique et al., 2021). However, if the aqueous and oil phases are inter dispersed, this is an indication of a bicontinuous μE (Scriven, 1976; Danielsson, 1981). An aim of the present study is to increase the bioavailability of BZD and improve the ophthalmic formulation for therapeutic relief to reduce intraocular pressure. In the present work, three new μE formulations were optimized using appropriate ratio of isopropyl myristate (IPM), water and 2-propanol, while Tween-80, Tween-20 and Tween-60 were selected as surfactant for each formulation respectively, to improve the solubility and load of BZD (basic molecular structure of BZD, Tween-20, Tween-60, Tween-80 are given in the Supplementary Material S1). By delineating the pseudoternary phase diagram and employing several complementary characterization techniques, optimal μE formulations were developed to upheld the appropriate amount of BZD, i.e., 2.0 wt%, 2.0 wt%, and 1.0 wt% in formulation A, B and C, respectively. The as-formulated smart template is a promising colloidal carrier for effective topical ocular administration of BZD with extended retention interval.

Materials and methods

Materials and chemicals

Isopropyl myristate (99.99%) and 2-propanol (99.99%) were purchased from Sigma-Aldrich, while Tween-80® (99.99%), Tween-60® (99.99%) and Tween-20® (99.99%) were purchased from VWR Chemicals. Schazoo Zaka Lab (PVT), Lahore, Pakistan, generously provided Brinzolamide (working standards). Distilled and deionized water was used for dilution.

Microemulsion formulation and mapping of ternary phase diagram

μEs of three different formulations were prepared using the titration method by mixing IPM as oil, 2-propanol as cosurfactant, Tween-80, Tween-20 and Tween-60 as surfactants. Surfactant/co-surfactant (S_{mix}) were used in a 1:1 ratio. Water was then added to form the optimized μE formulation. Formulation A consists of IPM, Tween-80, 2-propanol and water. Formulation B, on the other hand, comprised of IPM, Tween-20, 2-propanol and water. While, Formulation C consisted of IPM, Tween-60, 2-propanol and water. Ternary phase diagrams were constructed using random ratios of oil, water and S_{mix}. A dilution line AB as shown in Figure 1, was created at a constant S_{mix} ratio to investigate the structural changes of the μE from w/o to o/w phase. The optimal μEs were selected from the dilution line.

Incorporation of drug in μE

BZD was dissolved in each optimized μE formulation under continuous stirring at pH 7.2, 7.4 and 7.8 respectively at room temperature (30°C). Optimized μEs were consist of 38% Tween-80, 38% 2-propanol, 8% IPM and 16% water for formulation A, 40% Tween-20, 40% 2-propanol, 9% IPM and 11% water for formulation B and 40% Tween-60, 40% 2-propanol, 8% IPM and 12% water for formulation C μE A, B and C dissolved 2.0wt%, 2.0wt%, and 1.0wt% of BZD, respectively. All drug-free and drug-loaded optimal formulations were stable and transparent over 9 months of storage.

Characterization of microemulsion

Physical features, optical microscopic and stability study

The developed μE formulations were centrifuged for 15 min at 5,500 rpm using Hermle Z200 centrifuge equipment to check the

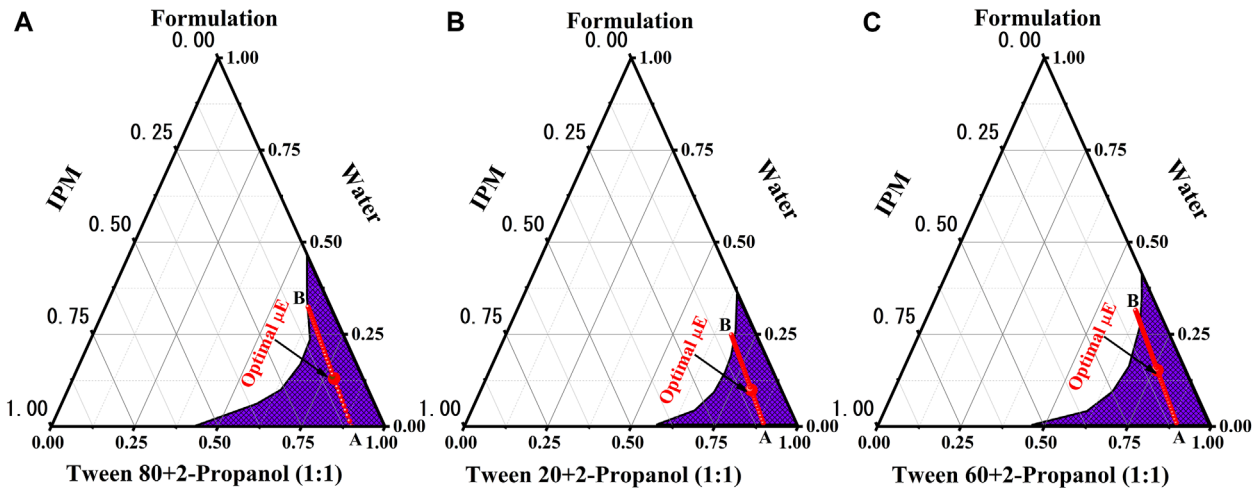

FIGURE 1
Pseudo ternary phase diagram of 2-propanol/Tween-80/Tween-20/Tween-60/IPM/oil/water for formulation **(A–C)**. **(A, B)** represents the dilution line. The highlighted dot on dilution line indicates the optimal µE.

stability of each drug-free and drug-loaded µE. Meanwhile, a biological microscope (LABOMED FLR Lx 400; Jenoptic, Germany) with 4x/10x/40x/×100 magnification was used to reveal the structural transitions in all drug free µE formulations. Viscosity was measured at 25°C ± 0.5°C with a calibrated Brookfield viscometer (LVDV-2T) at 150 rpm by washing and cleaning the viscometer at each measurement. Electrical conductivity measurement has been used to study and validate different types of phase inversion and continuous phase of µEs using a conductivity meter (ADWA AD-3000, Hungry).

Size distribution analysis

Using a Zetasizer (Malvern, Nano ZSP), the average droplet size of BZD-free and BZD-loaded formulation and the polydispersity index (PDI) were determined at room temperature without sample filtration. The equipment had a laser with a wavelength of 635 nm and backscattering technology, also known as NIBS (Non-Invasive Back-Scatter), was used to measure light scattering at an angle of 173°. For accuracy, each individual measurement was performed three times.

Spectroscopic measurements

The IR spectra of drug-free and drug-loaded µEs in the range of 500–4,000 cm^{-1} were recorded with a resolution of 2 cm^{-1} using a Bruker FTIR (Alpha series), while the steady-state fluorescence was measured using a spectrofluorophotometer (manufactured by Shimadzu RF-6000). The fluorescence spectra of BZD were recorded in the range of 300–800 nm. These spectra were recorded in aqueous phase, single oil phase, S_{mix} (1:1), and in each of the optimal µE systems.

In-Vitro drug release studies

The *in-vitro* release of all formulations was evaluated using simulated tear fluid (STF) at 50 rpm. The 2 mL freshly prepared STF medium used consisted of several salts, i.e.,; sodium chloride 0.65 g, sodium bicarbonate 0.25 g, calcium chloride dehydrate 0.009 g with 100 mL of water at a simulating eye temperature of 34°C ± 0.5°C. The fixed amount of all formulations, which was 1 g, was added into the dialysis membrane and sealed. The medium was sampled at the prescribed intervals (0, 5, 1, 2, 4, 8, 10, 12 and 24 h). An equal amount of STF medium was removed from it and added to maintain the volume, and the sinking condition was achieved. The BZD concentration in the retained samples was determined using the High performance liquid chromatography (HPLC) method.

HPLC analysis

The released BZD content was examined using HPLC. Briefly, 25 µL of solvent system was injected into the column before samples were diluted with the same volume. The column used was a C18 column (Zorbax SB, 4.6 mm250 cm, 5 m packing-L1, Agilent). Triethylamine phosphate buffer/acetonitrile/methanol was used as the mobile phase in a ratio of 70/20/10 v/v with a flow rate of 1.5 mL/min. The detector wavelength was 254 nm and the sample run time was approximately 10 min.

Results and discussions

Phase behaviour and physiochemical properties of µEs

The phase behavior of µE formulations consisting of oil, water and surfactant was studied using the ternary phase diagram as shown in Figure 1. Mapping the pseudoternary phase diagram is

TABLE 1 Physical Parameters of Optimal μEs.

Physical properties	Formulation-A IPM oil (8%), water (16%), Tween-80 (38%) and 2-propanol (38%)		Formulation-B IPM oil (9%), water (11%), Tween-20 (40%) and 2-propanol (40%)		Formulation-C IPM oil (8%), water (12%), Tween-60 (40%) and 2-propanol (40%)	
	BZD Free-μE	BZD Loaded-μE	BZD Free-μE	BZD Loaded-μE	BZD Free-μE	BZD Loaded-μE
Physical form	Light yellow transparent liquid	Light yellow transparent liquid	Light brown transparent liquid	Light brown transparent liquid	Light orange transparent liquid	Light orange transparent liquid
pH	7.2 ± 0.2	7.3 ± 0.3	7.4 ± 0.3	7.6 ± 0.3	7.8 ± 0.3	7.9 ± 0.4
Viscosity (cP)	396.5 ± 2.2	401.3 ± 3.0	338.3 ± 2.9	351.3 ± 3.6	367.3 ± 3.0	372.3 ± 4.0
Particle size DLS (nm)	26.3 ± 1.4	36.2 ± 2.5	45.3 ± 2.8	53.5 ± 2.5	36.5 ± 1.8	58.2 ± 2.3
Diffusion constant (cm^2/s)	4.19×10^{-10}	3.01×10^{-10}	2.85×10^{-10}	2.32×10^{-10}	3.26×10^{-10}	2.0×10^{-10}
ζ-potential (mV)	−32.9 ± 0.8	−34.8 ± 2.1	−30.7 ± 1.0	−35.2 ± 1.9	−35.4 ± 0.7	−36.7 ± 0.7
Stability	Over 9 months of storage					
FTIR	No renowned chemical intermolecular interaction among BZD and μE excipients					
Fluorescence	BZD most likely encapsulated in hydrophobic microenvironment					

important in formulating μEs (Rahman et al., 2017; Saleem et al., 2018). It enables the phase compatibility of the ingredients and the average area of μE formation to be determined. Different ratios of oil, S_{mix} and water were used (Lawrence and Rees, 2012; Subramanian et al., 2005; Rahdar et al., 2018). The behavior of each phase in the μE system was investigated through water dilution as this offers the advantages of fast, accurate and cost-effective operation at room temperature (Takamura et al., 1979). The present study comprised of oil (~8%), water (~16%), Tween-80 (~38%) and 2-propanol (~38%) as Formulation-A, oil (~9%), water (~11%), Tween-20 (~40%) and 2-propanol (~40%) as Formulation-B and oil (~8%), Water (~12%), Tween-60 (~40%) and 2-propanol (~40%) as Formulation-C. Figure 1 represents μE region (shaded area), while AB represent the dilution line and highlighted mark represents the optimal μE selected for further studies on physical stability based on the visual appearance for all formulations. The final formulation contained an excessive proportion of water compared to oil phase. This demonstrates the development of an o/w μE, as supported by previous studies (Saleem et al., 2019; Siddique et al., 2021). Table 1 lists some measured physical parameters of the optimal BZD-free μE and BZD-loaded μE of all μE sets.

Conductivity measurements

Electrical conductivity is convenient tool that determines the type of μE formed and the phase transitions of μE formation from water-in-oil (w/o) to oil-in-water (o/w) through the bicontinuous network channel (Yadav et al., 2018). μEs exhibit a sudden change in electrical conductivity when the composition is varied at a fixed temperature (Kahlweit et al., 1993). Figure 2 represents the changes in electrical conductivity for formulation A, B and C with increasing water content as a function of the weight fraction of the aqueous component (Φw) along the dilution line AB of the oil/S_{mix}. The bicontinuous channel of formulation A starts at ~16% Φ_w, which is called the percolation threshold (Φ_p), below this point the w/o μE at Φ_w < 16%. At a Φ_w value of 28%, the abrupt change occurs, indicating the formation of o/w μE with increasing water content and triggering the Φ_b phase transition (Pal et al., 2017; Nazar et al., 2018). As the Φ_w value increases, the first derivative ($d\sigma/d\varphi$) becomes even more helpful in determining the μE domain phase transition (Zavgorodnya et al., 2017). At Φ_w ~25%, the maximum value of the first derivative was observed, indicating the existence of a stable bicontinuous microstructure in this particular region.

Formulation-B showed the corresponding values of Φw for all suggested transitions in the microstructure are the percolation threshold (Φp ~ 21%), phase inversion (Φb ~ 36%), and bicontinuous channel ($d\sigma/d\Phi$ ~ 30%). Similarly the Formulation-C showed values of Φw for are the percolation threshold (Φp ~ 7%), phase inversion (Φb ~ 22%), and bicontinuous channel ($d\sigma/d\Phi$ ~ 15%).

Optical microscopic studies

An optical microscope was used to visualize the variations in microstructure of μE from w/o to o/w via a bicontinuous network channel. Microstructural transitions in μE were studied

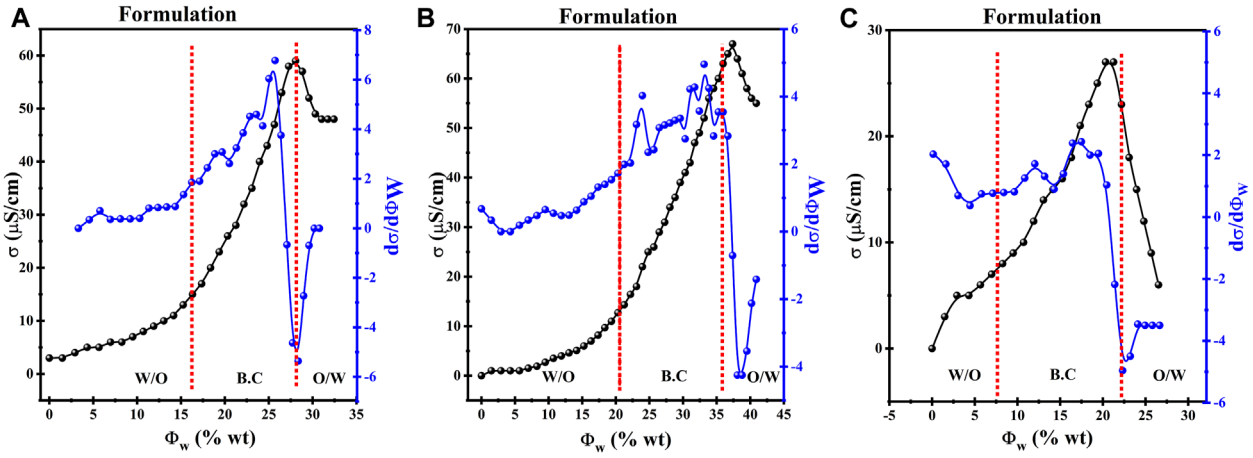

FIGURE 2
Discrepancy of electrical conductivity (σ) and the first derivative of the electric conductivity (do/dΦ) with Φ_w (wt%) alongside AB dilution line for BZD freeformulation **(A–C)**.

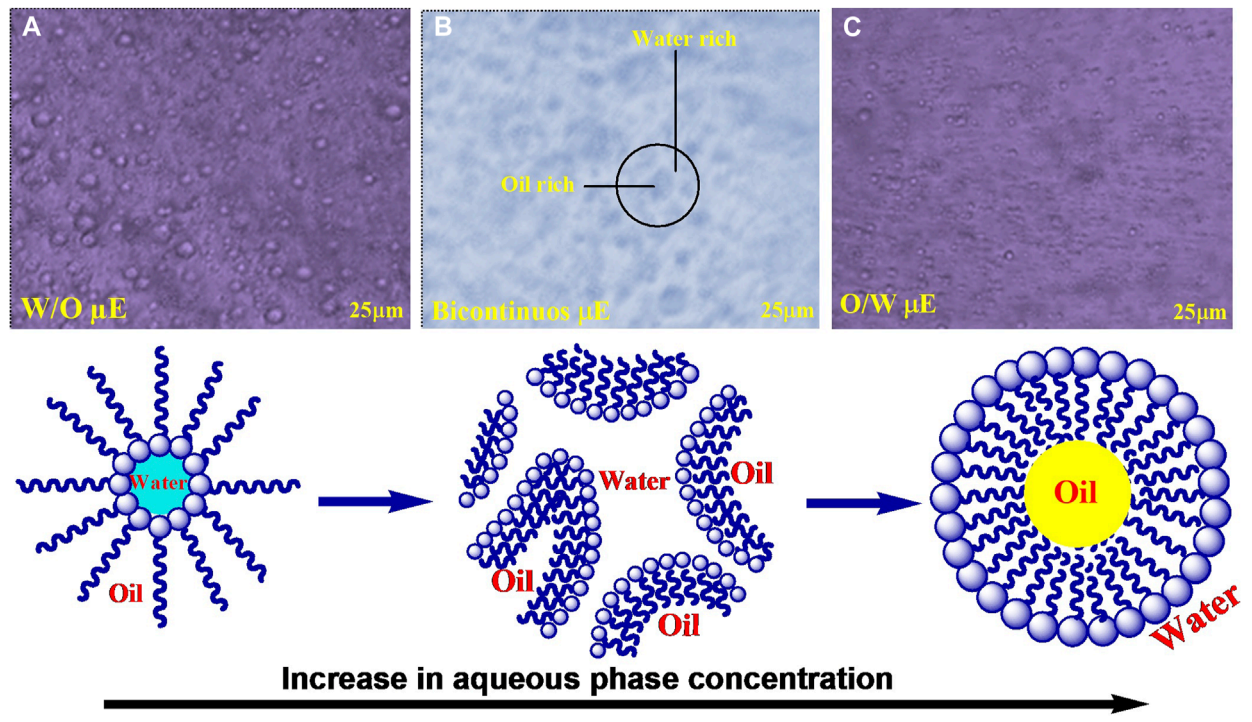

FIGURE 3
Optical micrographs of different types of the phase behavior on dilution of the μE **(A)** w/o μE; **(B)** bicontinuous μE; **(C)** o/w μE; along with the proposed microstructure variation.

under a biological microscope. The expected phase changes present in μE containing w/o, o/w, and bicontinuous network are shown along with the proposed microstructure, also sketched in Figure 3 (Nazar et al., 2020). Dispersed spherical oil and water droplets in their respective continuous phases constructing w/o and o/w μE are shown in Figures 3A, C respectively, while Figure 3B depicts a bicontinuous channel formed by a network of spherical droplets. The results agree well with previously reported observations by researchers (Nazar et al., 2018). The oil-rich composition showed the presence of μE with water droplets dispersed in the continuous oil phase (w/o), as shown in Figure 3A. Conversely, water-rich compositions exhibited μE with oil droplets dispersed in water (o/w), shown in Figure 3C. Between these two extremes, a bicontinuous μE emerged, revealing an aqueous phase-dependent microdomains, as shown in Figure 3B. The distinctive microstructures are influenced by the

hydrophilic-lipophilic balance (HLB) value of surfactant and co-surfactant (Paria and Khilar, 2000; Rahdar et al., 2018; Qadri et al., 2022b). When the HLB leans towards the hydrophilic side, a two-layer o/w system is formed in which oil is dispersed in the water phase and *vice versa* (Khan et al., 2016). For μEs in which neither water nor oil droplets form, the term bicontinuous emerged, signifying the percolation behavior (Dasilva-Carvalhal et al., 2003; Rahman et al., 2016).

Size distribution analysis

Size distribution analysis of BZD-free and BZD-loaded μE of all formulations was performed to check the stability of the dispersed partciles using dynamic light scattering (DLS) (Khan et al., 2016). As shown in Figure 4, the particle size of BZD-free μE droplet was 26.3 ± 1.4, 45.3 ± 2.8 and 36.5 ± 1.8 nm for formulation A, B and C, respectively each represented monostructured droplets by a single peak (Soomro et al., 2016). When BZD was loaded into the μE, the average partcile size increased to 36.2 ± 2.5, 53.5 ± 2.5 and 58.2 ± 2.3 nm for formulation A, B and C respectively, indicating the accumulation and encapsulation of BZD inside the interfacial layers of microstructres (Richard et al., 2017; Xiang et al., 2023). The low polydispersity index (PDI <0.3) indicates uniform homogeneity of the droplet distribution of the μE formulation (Khan et al., 2016). Furthermore, the negative ζ-potential values indicated the high colloidal stability, as the highly stable μE has a ζ-potential value of either >30 mV or < −30 mV due to the electrostatic repulsion between the droplets (Nazar et al., 2017; Pavoni et al., 2020). Other researchers have found and reported similar results (Nazar et al., 2018; Siddique et al., 2024). The values of diffusion coefficients D) are listed in Table 1, which were calculated using the Stokes–Einstein relationship ($D = \frac{k_B T}{6\pi\eta r}$) at a temperature of 298 K (where r is the hydrodynamic radius of droplets). The higher D value for μE indicated greater diffusion across the membrane barriers, while lower D values show longer retention and are therefore considered responsible for sustained permeation (Erdal et al., 2016; Nakamura et al., 2016; Nazar et al., 2018).

FTIR analysis

FTIR analysis was performed to check the compatibility of BZD with μE excipients. The FTIR spectra of pure drug, BZD-free and BZD-loaded μE of all formulation are shown in Figure 5. In the FTIR spectrum of pure BZD drug, a signal in the range of 3,110–3,350 cm^{-1} was observed, probably due to N–H stretching vibrations, while a weak peak in the range of 3,100–3,000 cm^{-1} is attributed to the C–H stretching mode. The peak observed at 1,644 cm^{-1} was due to the asymmetric and symmetric C–C stretching vibrations, while a strong band at 1,450 cm^{-1} corresponds to the bending of the C–H bond. The FTIR spectrum of the BZD-loaded μE is completely different from that of the BZD-pure powder; however the spectrum of BZD-free μE and BZD-loaded μE showed no significant change in all formulations, indicating that no interaction with μE excipients could be observed, demonstrating the stability of BZD within the microstructures (Schneider et al., 2011; Dinache et al., 2020).

The FTIR spectrum of BZD-loaded μE demonstrates that the BZD is completely dissolved in μE and the peak-to-peak correlation showed that there are no larger aggregates due to the absence

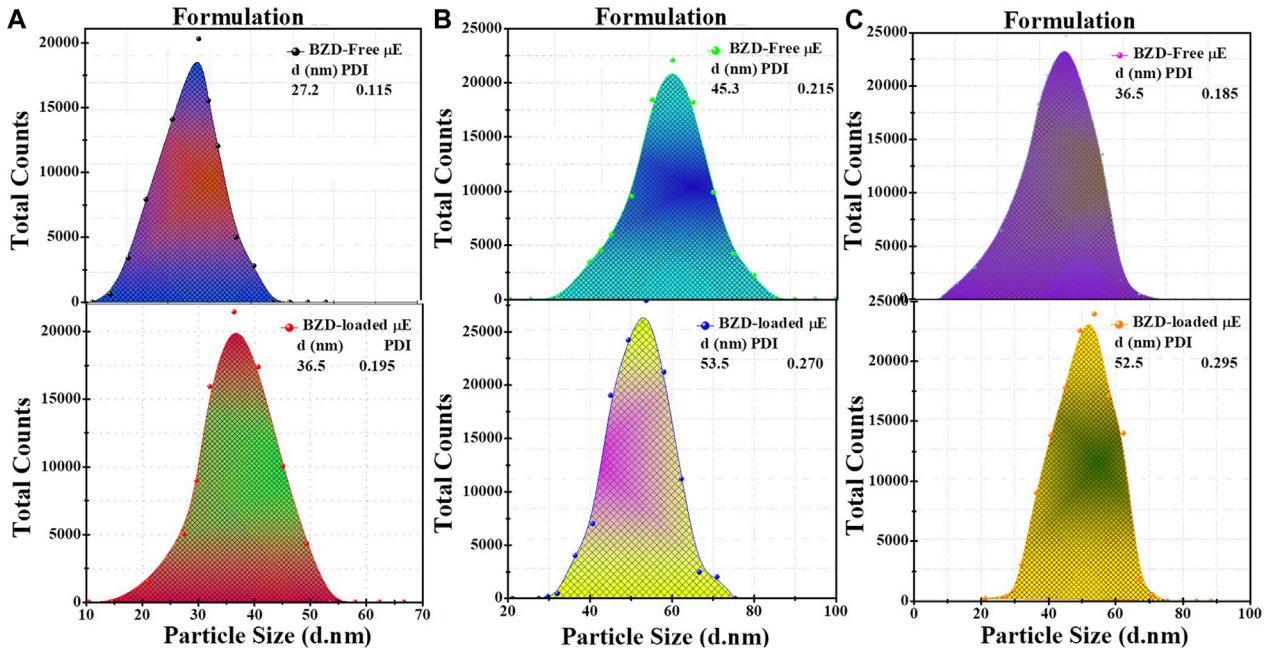

FIGURE 4
Particle size distribution of BZD-free μE, BZD-loaded μE of formulation **(A–C)** respectively analyzed by DLS.

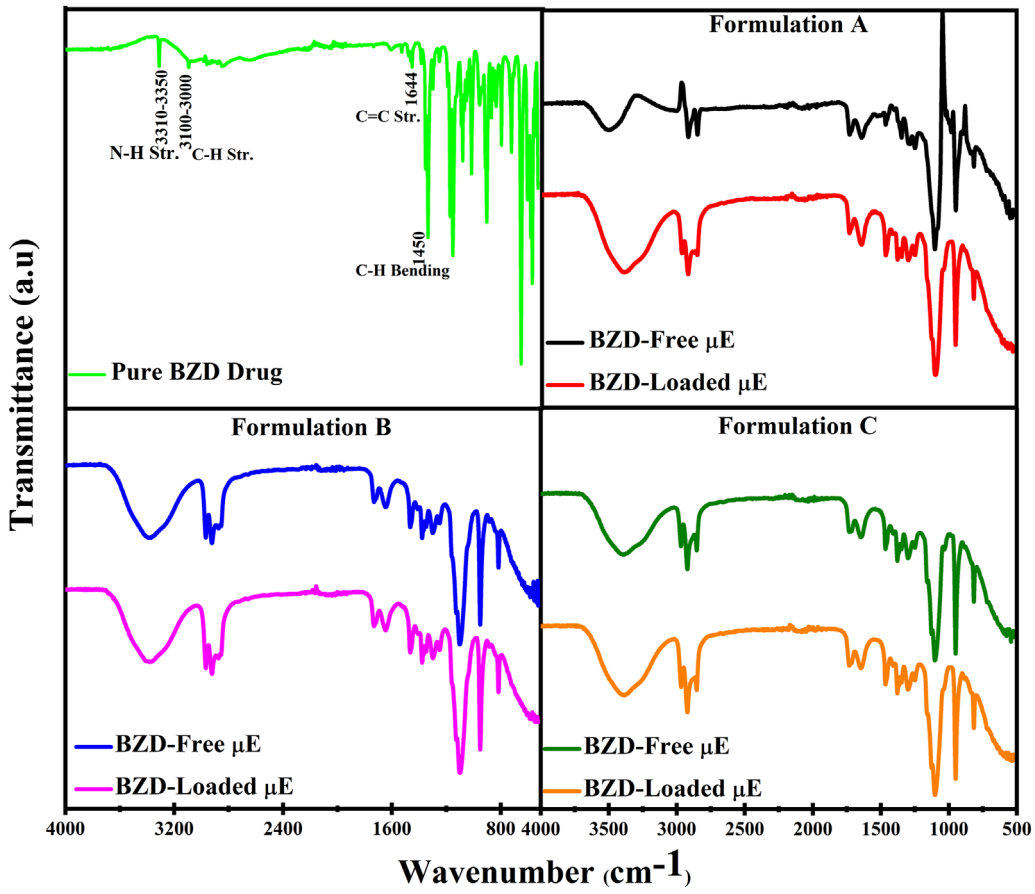

FIGURE 5
FTIR spectra of pure BZD drug, BZD-free µE, BZD-loaded µE, of formulation **(A–C)** respectively.

of any additional peak (Nazar et al., 2009). However, some slight changes in intensities are observed, which are most likely due to the different molecular environments experienced by BZD in different µE formulations due to the weak physical interactions such as hydrogen bonding or intermolecular forces between the functional groups of the BZD and excipients (Saleem et al., 2019). However, these connections may facilitate sustained release of the BZD.

Fluorescence studies

The steady-state spectrophotometry is widley used to measure the partioning of the drug in microdomains of the µE as it depends on the polarity of medium provided (Lissi et al., 2000; Pal et al., 2011). The emission spectra of BZD in water, IPM, S_{mix} of all formulations are depicted in Figure 6. The maximum emission (λ_{em}) of BZD in water was observed at 345 nm, while in IPM it was at 360 nm. The λ_{em} of BZD in S_{mix} A, B and C were at 422 nm, 456 nm and 465 nm, while the λ_{em} of optimal µE-A, µE-B and µE-C was at 408 nm, 406 nm and 404 nm. A red shift was observed in S_{mix} and optimal µE formulations as compared to water. These results suggests that BZD molecules are firmly contained to the non-polar portion of the interface and are shielded by any pure bulk domain, such as water or oil (Pal et al., 2011). All of these results indicate that micro-aggregate-assembled probes may be found close to the µE interface, where excitation propagation was inhibited and additive rotation is further limited (Nazar et al., 2020; Saleem et al., 2020).

In-Vitro drug release study

New formulations are created and their efficacy is examined in term of *in-vitro* release also an effort to reduce the use of animal models (Bachhav and Patravale, 2009; Yasir Siddique et al., 2021). The *in-vitro* release of BZD from µE was assessed by STF as a release medium that simulated the ocular environment after several interval of time (Wu et al., 2013). The release of BZD was found >99.9% of formulation A in interval of 10 h, while the interval for the formulation B and C was 4 and 7 h demonstrating faster release than formulation A owing various factors, such as viscosity, surfactant, oil phase and drug solubility which can affect the release rate (Siafaka et al., 2015). 2-Propanol tends to lower the surface tension of the surfactant ultimately enhances the drug release as it makes the surface of droplet smooth and dynamic (Figueiredo et al., 2016). In Figure 7, the release rate of BZD from all three optimal µE has shown different BZD release at different time due to change in surfactant. In start, all µE showed a slow release of BZD until

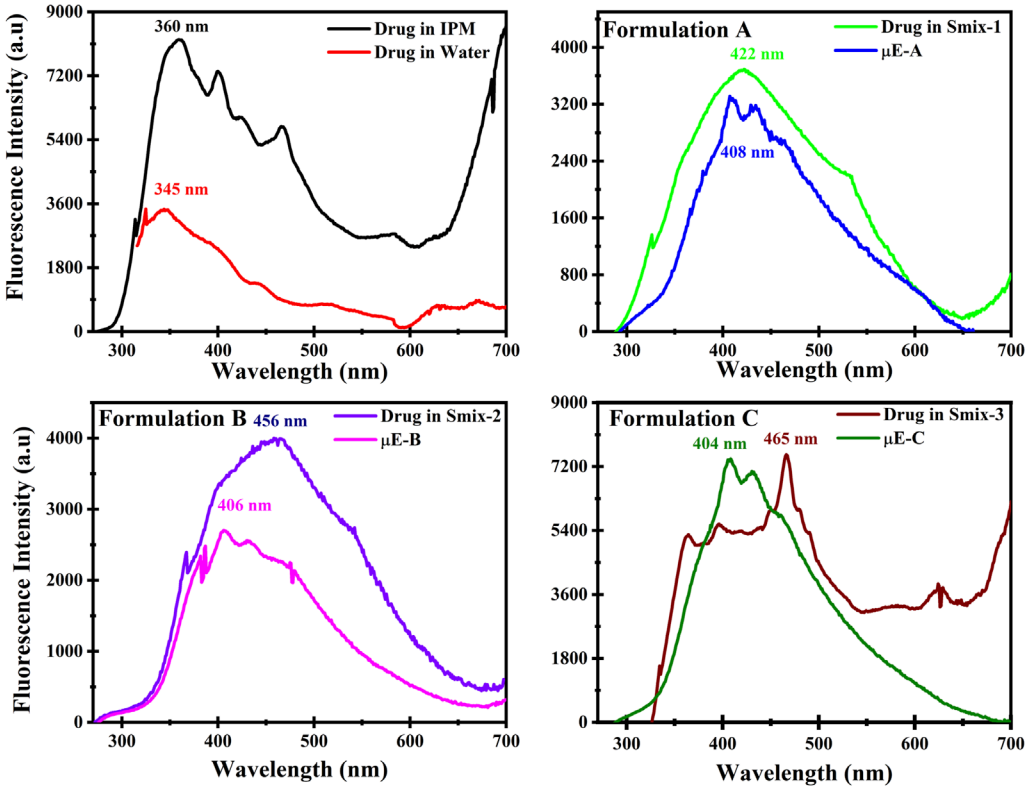

FIGURE 6
Fluorescence spectrum of drug in isopropyl myristate (IPM), drug in water, drug in S_{mix} and in optimal μE formulations **(A–C)** respectively.

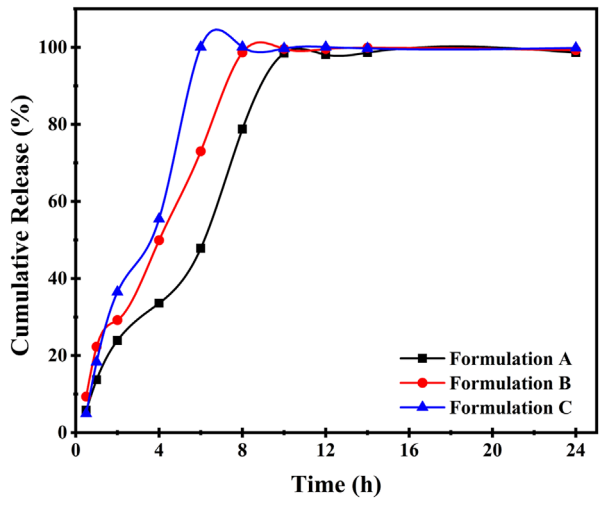

FIGURE 7
In vitro release studies of prepared μE containing BZD of Formulation **(A–C)** during 0–24 h.

5 h. After that a sudden increase in release rate has been observed (Siafaka et al., 2021).

Formulation A showed ~35% BZD release at 4 h and rest of the 60% get released round about 10 h. In formulation B, 50% BZD was released at 4 h and rest of the BZD was released at 8 h, similar trend was followed by formulations C. Additionally, formulation A showed a sustained release in 10 h among all 3 μE formulation indicating lower dosage quantity because of sustained release.

Conclusion

Three new formulations were made which were consist of formulation A of Tween-80, 2-propanol, IPM and water, formulation B of Tween-20, 2-propanol, IPM and water and formulation C of Tween-60, 2-propanol, IPM and water to enhance the solubility and bioavailability of the antihypertensive drug BZD. Transformation of phases in μE was studied through electrical conductivity, microscopic images and viscosity measurements. To check the stability and presence of BZD fluorescence and DLS study was done. The findings show that BZD-loaded μE with low and desirable thin globule sizes were successfully generated. Evidently, the developed optimized microemulsions can be used as ocular carriers for glaucoma therapy; nevertheless, formulation A, which contained Tween-80/2-propanol as the surfactant, cosurfactant, IPM as the oil phase, was the most ideal of all. In actuality, formulation A offers superior physicochemical values and delayed release, which are both noteworthy benefits. Traditional topical treatments can be expensive, but this new technology may offer some benefits, making it more affordable and sustainable in the long term.

Data availability statement

The original contributions presented in the study are included in the article/Supplementary Material, further inquiries can be directed to the corresponding authors.

Author contributions

SZ: Conceptualization, Formal Analysis, Investigation, Methodology, Software, Writing–original draft. MN: Conceptualization, Funding acquisition, Project administration, Supervision, Writing–original draft, Writing–review and editing. MS: Formal Analysis, Methodology, Software, Writing–review and editing. SH: Data curation, Formal Analysis, Methodology, Writing–review and editing. KA: Formal Analysis, Methodology, Writing–review and editing. MS: Formal Analysis, Methodology, Software, Writing–review and editing. SS: Formal Analysis, Writing–review and editing. HA: Formal Analysis, Software, Writing–review and editing. ZU: Formal Analysis, Funding acquisition, Software, Supervision, Writing–review and editing.

Funding

The author(s) declare that financial support was received for the research, authorship, and/or publication of this article. The research work was supported by project #RSP 2024R399, King Saud University, Riyadh, Saudi Arabia.

Acknowledgments

The author, MN, express their gratitude to the Higher Education Commission of Pakistan for providing financial support through NRPU Project No. 20-17321/NRPU/R&D/HEC/2021. The authors sincerely appreciate funding from Researchers Supporting Project number (RSP 2024R399), King Saud University, Riyadh, Saudi Arabia. Furthermore, the authors express their appreciation to the Department of Chemistry, University of Education, Multan Campus, Pakistan and the Department of Chemical Engineering, King Saud University, Saudi Arabia for providing laboratory facilities to conduct their research.

Conflict of interest

The authors declare that the research was conducted in the absence of any commercial or financial relationships that could be construed as a potential conflict of interest.

The author(s) declared that they were an editorial board member of Frontiers, at the time of submission. This had no impact on the peer review process and the final decision.

Publisher's note

Supplementary material

The Supplementary Material for this article can be found online at: https://www.frontiersin.org/articles/10.3389/fmats.2024.1363138/full#supplementary-material

References

Abd El Wahab, L. M., Essa, E. A., El Maghraby, G. M., and Arafa, M. F. (2022). The development and evaluation of phase transition microemulsion for ocular delivery of acetazolamide for glaucoma treatment. *AAPS PharmSciTech* 24 (1), 1. doi:10.1208/s12249-022-02459-7

Bachhav, Y. G., and Patravale, V. B. (2009). Microemulsion based vaginal gel of fluconazole: formulation, *in vitro* and *in vivo* evaluation. *Int. J. Pharm.* 365 (1), 175–179. doi:10.1016/j.ijpharm.2008.08.021

Choradiya, B. R., and Patil, S. B. (2022). Design, development, and characterization of brinzolamide and brimonidine tartrate nanoemulsion for ophthalmic drug delivery. *Thai J. Pharm. Sci.* 46 (4), 413–424.

Constantinides, P. P. (1995). Lipid microemulsions for improving drug dissolution and oral absorption: physical and biopharmaceutical aspects. *Pharm. Res.* 12, 1561–1572. doi:10.1023/a:1016268311867

Danielsson, I. (1981). The definition of microemulsion. *Colloids Surfaces* 3 (4), 391–392. doi:10.1016/0166-6622(81)80064-9

Dasilva-Carvalhal, J., García-Río, L., Gómez-Díaz, D., Mejuto, J. C., and Rodríguez-Dafonte, P. (2003). Influence of crown ethers on the electric percolation of AOT/isooctane/water (w/o) microemulsions. *Langmuir* 19 (15), 5975–5983. doi:10.1021/la026857m

Dinache, A., Tozar, T., Smarandache, A., Andrei, I. R., Nistorescu, S., Nastasa, V., et al. (2020). Spectroscopic characterization of emulsions generated with a new laser-assisted device. *Molecules* 25 (7), 1729. doi:10.3390/molecules25071729

Eissa, M. (2016). Validated spectrophotometric methods for simultaneous determination of brinzolamide and timolol maleate in their pure form and ophthalmic preparation. *Al-Azhar J. Pharm. Sci.* 54 (1), 188–202. doi:10.21608/ajps.2018.6643

Erdal, M. S., Özhan, G., Mat, C., Özsoy, Y., and Güngör, S. (2016). Colloidal nanocarriers for the enhanced cutaneous delivery of naftifine: characterization studies and *in vitro* and *in vivo* evaluations. *Int. J. nanomedicine* 11, 1027–1037. doi:10.2147/ijn.s96243

Figueiredo, K. A., Neves, J. K. O., Silva, J. A. d., Freitas, R. M. d., and Carvalho, A. L. M. (2016). Phenobarbital loaded microemulsion: development, kinetic release and quality control. *Braz. J. Pharm. Sci.* 52, 251–264. doi:10.1590/s1984-82502016000200003

Gasco, M. (1997). Microemulsions in the pharmaceutical field: perspectives and applications. *Surfactant Sci. Ser.* 66, 97–122.

Gohil, R., (2020). Optimization of brinzolamide loaded microemulsion using formulation by design approach: characterization and *in-vitro* evaluation. *Curr. Drug Ther.* 15 (1), 37–52. doi:10.2174/22123903otu1zotc6tcvy

Grampurohit, N., Ravikumar, P., and Mallya, R. (2011). Microemulsions for topical use–a review. *Ind. J. Pharm. Edu Res.* 45 (1), 100–107.

Kahlweit, M., Busse, G., and Winkler, J. (1993). Electric conductivity in microemulsions. *J. Chem. Phys.* 99 (7), 5605–5614. doi:10.1063/1.465953

Kantaria, S., Rees, G. D., and Lawrence, M. J. (2003). Formulation of electrically conducting microemulsion-based organogels. *Int. J. Pharm.* 250 (1), 65–83. doi:10.1016/s0378-5173(02)00491-x

Khan, M. F., Singh, M. K., and Sen, S. (2016). Measuring size, size distribution, and polydispersity of water-in-oil microemulsion droplets using fluorescence correlation spectroscopy: comparison to dynamic light scattering. *J. Phys. Chem. B* 120 (5), 1008–1020. doi:10.1021/acs.jpcb.5b09920

Lawrence, M. J., and Rees, G. D. (2012). Microemulsion-based media as novel drug delivery systems. *Adv. drug Deliv. Rev.* 64, 175–193. doi:10.1016/j.addr.2012.09.018

Lissi, E., Abuin, E. B., Rubio, M. A., and Cerón, A. (2000). Fluorescence of Prodan and Laurdan in AOT/heptane/water microemulsions: partitioning of the probes and characterization of microenvironments. *Langmuir* 16 (1), 178–181. doi:10.1021/la990720n

Loiselle, A. R., de Kleine, E., van Dijk, P., and Jansonius, N. M. (2020). Intraocular and intracranial pressure in glaucoma patients taking acetazolamide. *PLoS One* 15 (6), e0234690. doi:10.1371/journal.pone.0234690

Nakamura, Y., Mochida, A., Choyke, P. L., and Kobayashi, H. (2016). Nanodrug delivery: is the enhanced permeability and retention effect sufficient for curing cancer? *Bioconjugate Chem.* 27 (10), 2225–2238. doi:10.1021/acs.bioconjchem.6b00437

Narang, A. S., Delmarre, D., and Gao, D. (2007). Stable drug encapsulation in micelles and microemulsions. *Int. J. Pharm.* 345 (1-2), 9–25. doi:10.1016/j.ijpharm.2007.08.057

Nazar, M. F., Khan, A. M., and Shah, S. S. (2009). Microemulsion system with improved loading of piroxicam: a study of microstructure. *AAPS PharmSciTech* 10 (4), 1286. doi:10.1208/s12249-009-9328-9

Nazar, M. F., Mujeed, A., Siddique, M. Y., Zafar, M., Saleem, M. A., Khan, A. M., et al. (2020). Structural dynamics of tween-based microemulsions for antimuscarinic drug mirabegron. *Colloid Polym. Sci.* 298 (3), 263–271. doi:10.1007/s00396-020-04603-w

Nazar, M. F., Saleem, M. A., Bajwa, S. N., Yameen, B., Ashfaq, M., Zafar, M. N., et al. (2017). Encapsulation of antibiotic levofloxacin in biocompatible microemulsion formulation: insights from microstructure analysis. *J. Phys. Chem. B* 121 (2), 437–443. doi:10.1021/acs.jpcb.6b09326

Nazar, M. F., Yasir Siddique, M., Saleem, M. A., Zafar, M., Nawaz, F., Ashfaq, M., et al. (2018). Fourth-generation antibiotic gatifloxacin encapsulated by microemulsions: structural and probing dynamics. *Langmuir* 34 (36), 10603–10612. doi:10.1021/acs.langmuir.8b01775

Pal, N., Saxena, N., and Mandal, A. (2017). Phase behavior, solubilization, and phase transition of a microemulsion system stabilized by a novel surfactant synthesized from castor oil. *J. Chem. Eng. Data* 62 (4), 1278–1291. doi:10.1021/acs.jced.6b00806

Pal, N., Verma, S. D., Singh, M. K., and Sen, S. (2011). Fluorescence correlation spectroscopy: an efficient tool for measuring size, size-distribution and polydispersity of microemulsion droplets in solution. *Anal. Chem.* 83 (20), 7736–7744. doi:10.1021/ac2012637

Paria, S., and Khilar, K. (2000). Microemulsion-based media as novel drug delivery systems. *Adv. Drug Deliv. Rev.* 45, 89–121. doi:10.1016/s0169-409x(00)00103-4

Patel, A., (2013). Ocular drug delivery systems: an overview. *World J. Pharmacol.* 2 (2), 47. doi:10.5497/wjp.v2.i2.47

Pavoni, L., Perinelli, D. R., Bonacucina, G., Cespi, M., and Palmieri, G. F. (2020). An overview of micro- and nanoemulsions as vehicles for essential oils: formulation, preparation and stability. *Nanomaterials* 10 (1), 135. doi:10.3390/nano10010135

Qadri, H. K., Shaheen, A., Rashid, S., Ahmad Bhat, I., Mohammad Rather, G., and Ahmad Dar, A. (2022a). Micellization and gelation characteristics of Pluronic P123 and single ester-bonded cleavable cationic gemini surfactant: a potential system for solubilization and release of ibuprofen. *J. Mol. Liq.* 366, 120311. doi:10.1016/j.molliq.2022.120311

Qadri, H. K., Shaheen, A., Rashid, S., Ahmad Bhat, I., Mohammad Rather, G., and Ahmad Dar, A. (2022b). Micellization and gelation characteristics of Pluronic P123 and single ester-bonded cleavable cationic gemini surfactant: a potential system for solubilization and release of ibuprofen. *J. Mol. Liq.* 366, 120311. doi:10.1016/j.molliq.2022.120311

Rahdar, A., Almasi-Kashi, M., Khan, A. M., Aliahmad, M., Salimi, A., Guettari, M., et al. (2018). Effect of ion exchange in NaAOT surfactant on droplet size and location of dye within Rhodamine B (RhB)-containing microemulsion at low dye concentration. *J. Mol. Liq.* 252, 506–513. doi:10.1016/j.molliq.2018.01.004

Rahman, A., Rahman, M. M., Mollah, M. Y. A., and Susan, M. A. B. H. (2016). Dynamic percolation and swollen behavior of nanodroplets in 1-ethyl-3-methylimidazolium trifluoromethanesulfonate/triton X-100/cyclohexane microemulsions. *J. Phys. Chem. B* 120 (28), 6995–7002. doi:10.1021/acs.jpcb.6b04763

Rahman, H. M. A. U., Afzal, S., Nazar, M. F., Alvi, D. A., Khan, A. M., and Asghar, M. N. (2017). Phase behavior of a TX-100/oleic acid/water based ternary system: a microstructure study. *J. Mol. Liq.* 230, 15–19. doi:10.1016/j.molliq.2017.01.011

Richard, B., Lemyre, J.-L., and Ritcey, A. M. (2017). Nanoparticle size control in microemulsion synthesis. *Langmuir* 33 (19), 4748–4757. doi:10.1021/acs.langmuir.7b00773

Saleem, M., Nazar, M. F., Yameen, B., Khan, A. M., Hussain, S. Z., and Khalid, M. R. (2018). Structural insights into the microemulsion-mediated formation of fluoroquinolone nanoantibiotics. *ChemistrySelect* 3, 11616–11621. doi:10.1002/slct.201801925

Saleem, M. A., (2023). "Chapter 11 - self-nanoemulsifying drug delivery systems with bioavailability potential," in *Novel platforms for drug delivery applications*. Editors S. Das, S. Thomas, and P. P. Das (Woodhead Publishing, England, UK), 257–275.

Saleem, M. A., Yasir Siddique, M., Nazar, M. F., Khan, S. U. D., Ahmad, A., Khan, R., et al. (2020). Formation of antihyperlipidemic nano-ezetimibe from volatile microemulsion template for enhanced dissolution profile. *Langmuir* 36 (27), 7908–7915. doi:10.1021/acs.langmuir.0c01016

Saleem, M. N., Nazar, M. F., Siddique, M. Y., Khan, A., Ashfaq, M., Hussain, S. Z., et al. (2019). Soft-templated fabrication of antihypertensive nano-Irbesartan: structural and dissolution evaluation. *J. Mol. Liq.* 292, 111388. doi:10.1016/j.molliq.2019.111388

Schneider, C., Hanisch, M., Wedel, B., Jusufi, A., and Ballauff, M. (2011). Experimental study of electrostatically stabilized colloidal particles: colloidal stability and charge reversal. *J. Colloid Interface Sci.* 358 (1), 62–67. doi:10.1016/j.jcis.2011.02.039

Scriven, L. E. (1976). Equilibrium bicontinuous structure. *Nature* 263 (5573), 123–125. doi:10.1038/263123a0

Siafaka, P. I., Çağlar, E. Ş., Sipahi, H., Charehsaz, M., Aydın, A., and Üstündağ Okur, N. (2021). Ocular microemulsion of brinzolamide: formulation, physicochemical characterization, and *in vitro* irritation studies based on EpiOcular™ eye irritation assay. *Pharm. Dev. Technol.* 26 (7), 765–778. doi:10.1080/10837450.2021.1944206

Siafaka, P. I., Titopoulou, A., Koukaras, E. N., Kostoglou, M., Koutris, E., Karavas, E., et al. (2015). Chitosan derivatives as effective nanocarriers for ocular release of timolol drug. *Int. J. Pharm.* 495 (1), 249–264. doi:10.1016/j.ijpharm.2015.08.100

Siddique, M. Y., Alamgir, I., Nazar, M. F., Sumrra, S. H., Ashfaq, M., Safdar, M., et al. (2021). Structural and probing dynamics of Brij-35-based microemulsion for fluoroquinolone antibiotics. *Colloid Polym. Sci.* 299 (9), 1479–1488. doi:10.1007/s00396-021-04871-0

Siddique, M. Y., Nazar, M. F., Saleem, M. A., Haider, S., Sumrra, S. H., Akhtar, M. S., et al. (2024). Formulation of gelled microemulsion for effective permeation of celecoxib across the skin barrier. *ChemistrySelect* 9 (3), e202302841. doi:10.1002/slct.202302841

Silver, L. H., and Group, B. C. S. (2000). Ocular comfort of brinzolamide 1.0% ophthalmic suspension compared with dorzolamide 2.0% ophthalmic solution: results from two multicenter comfort studies. *Surv. Ophthalmol.* 44, S141–S145. doi:10.1016/s0039-6257(99)00111-3

Soomro, R., Memon, N., Bhanger, M. I., and Denizli, A. (2016). Horseradish peroxidase immobilized into organogel-silica composite for transformation of chlorophenols to biodegradable organic acids. *Hacettepe J. Biol. Chem.* 44 (3), 361–374. doi:10.15671/hjbc.20164420579

Subramanian, N., Ghosal, S. K., Acharya, A., and Moulik, S. P. (2005). Formulation and physicochemical characterization of microemulsion system using isopropyl myristate, medium-chain glyceride, polysorbate 80 and water. *Chem. Pharm. Bull.* 53 (12), 1530–1535. doi:10.1248/cpb.53.1530

Takamura, A., Minowa, T., Noro, S., and Kubo, T. (1979). Effects of tween and span group emulsifiers on the stability of o/w emulsions. *Chem. Pharm. Bull.* 27 (12), 2921–2926. doi:10.1248/cpb.27.2921

Tenjarla, S. (1999). Microemulsions: an overview and pharmaceutical applications. *Crit. Reviews™ Ther. Drug Carr. Syst.* 16 (5), 62. doi:10.1615/critrevtherdrugcarriersyst.v16.i5.20

Urtti, A. (2006). Challenges and obstacles of ocular pharmacokinetics and drug delivery. *Adv. drug Deliv. Rev.* 58 (11), 1131–1135. doi:10.1016/j.addr.2006.07.027

Wu, W., Li, J., Wu, L., Wang, B., Wang, Z., Xu, Q., et al. (2013). Ophthalmic delivery of brinzolamide by liquid crystalline nanoparticles: *in vitro* and *in vivo* evaluation. *Aaps Pharmscitech* 14, 1063–1071. doi:10.1208/s12249-013-9997-2

Xiang, H., Xu, S., Zhang, W., Li, Y., Zhou, Y., and Miao, X. (2023). Skin permeation of curcumin nanocrystals: effect of particle size, delivery vehicles, and permeation enhancer. *Colloids Surfaces B Biointerfaces* 224, 113203. doi:10.1016/j.colsurfb.2023.113203

Yadav, V., Jadhav, P., Kanase, K., Bodhe, A., and Dombe, S. (2018). Preparation and evaluation of microemulsion containing antihypertensive drug. *Int. J. Appl. Pharm.* 10 (5), 138–146. doi:10.22159/ijap.2018v10i5.27415

Yasir Siddique, M., Nazar, M. F., Mahmood, M., Saleem, M. A., Alwadai, N., Almuslem, A. S., et al. (2021). Microemulsified gel formulations for topical delivery of clotrimazole: structural and *in vitro* evaluation. *Langmuir* 37 (46), 13767–13777. doi:10.1021/acs.langmuir.1c02590

Yuan, Y., Li, S. m., Mo, F. k., and Zhong, D. f. (2006). Investigation of microemulsion system for transdermal delivery of meloxicam. *Int. J. Pharm.* 321 (1-2), 117–123. doi:10.1016/j.ijpharm.2006.06.021

Zavgorodnya, O., Carmona-Moran, C. A., Kozlovskaya, V., Liu, F., Wick, T. M., and Kharlampieva, E. (2017). Temperature-responsive nanogel multilayers of poly(N-vinylcaprolactam) for topical drug delivery. *J. Colloid Interface Sci.* 506, 589–602. doi:10.1016/j.jcis.2017.07.084